Journal of Scientific & Industrial Research
Vol. 85, April 2026, pp. 291-300
DOI: 10.56042/jsir.v85i4.20640

Novel Biomaterial based Nanocomposite Coating for Corrosion Inhibition Studies of Carbon Steel

Sara Al-Shibli[1], Geetha Devi[1]*, Athari Al-Badi[1], Aravind N[2] & Ola Al-Dhabari[1]

[1]Department of Mechanical & Industrial Engineering,

[2]Department of Civil & Environmental Engineering, College of Engineering, National University of Science & Technology, Oman

Received 13 June 2025; revised 22 January 2026; accepted 13 May 2026

Corrosion is a rising concern in oil and gas sectors, which causes destruction of the material and results in heavy financial loss accompanied by high risk to human health and safety. This study investigates the corrosion inhibition efficiency of a novel biomaterial based nanostructured coating on carbon steel specimen by dip-coating technique using *Ziziphus Spina* leaf extract, silica nanoparticles (SiO_2NPs), and biopolymer (chitosan) matrix. The anti-corrosion performance of the fabricated composite thin film was investigated by exposing the coated specimen at different environmental conditions and the effectiveness was examined using potentiostatic, weight loss measurement, atmosphere and wet/dry tests. The main characterization tools employed are Atomic force microscopy (AFM), X-ray diffraction (XRD), Fourier transform infrared spectroscopy (FTIR), and Field emission scanning electron microscopy (FE-SEM). Tafal plot was used to study the corrosion rate. The results of atomic-level micro structural analysis performed by FE-SEM and AFM suggested the successful development of inhibitor layer at the carbon steel surface to prevent the corrosion. The experimental outcomes underscore the potential of biomaterial based nanostructured coating as an effective corrosion inhibitor for carbon steel in acidic environments. The nanocomposite thin films act as an efficient protective coating and offers superior corrosion resistance with extended lifespan of the carbon steel. The study validates that the green corrosion inhibitors developed from natural resources with minimum layer thickness could be a realistic solution in regulating the corrosion in oil pipelines with improved corrosion resistance, exceptional chemical stability, durability, and improved strength.

Keywords: Atomic force microscopy, Chitosan, Corrosion protection, Dipcoating, Green inhibitor

Introduction

Corrosion problems are the most serious issue in the oil and gas industries, which results in massive monetary loss due to deterioration of metal surface and damage to the industrial equipment and oil pipelines. The publication of National Association of Corrosion Engineers (NACE) demonstrates the global corrosion cost is nearly 2.5 trillion USD, which is expected to be 3.5% of the world's GDP. This imposes a strong corrosion control strategy to lessen the mounting challenges and reduce operational overheads over the long-term strategy. In the year 2024, the production of crude oil and condensates escalate by 10%. Corrosion problem result in massive financial liability and safety risks due to the destruction of material and hence damages the oil pipelines. The oil and gas sector in the Sultanate of Oman supplements 44% of the GDP.[1,2] The corrosion reaction results in rust formation on steel surface and possesses significant challenges to industrial operations. The deterioration of the oil pipelines is due to the interaction with the corrosive environment and chemicals containing CO_2, sodium chloride, H_2S, water, and chlorine compounds.[3] This results in safety and health risks leading to chemical hazard, equipment damage, unplanned maintenance, environmental distress, and huge financial liability. Corrosion problems also lead to reduced service life of industrial process equipment, which interrupt the flow passage through the pipeline and spoil the pumps and valves.[4] The pitting corrosion, uniform corrosion, crevice corrosion, galvanic corrosion; stress corrosion, and selective corrosion, etc leads to huge liability to industries.[5] Therefore, it is indispensable to protect the assets and minimize the global annual outflow to lessen corrosion issues warranting the durability and reliability of equipment.

Protection of coated metallic surfaces will improve the barrier properties of the metal surface, and it has

*Author for Correspondence
E-mail: geethadevi@nu.edu.om

been considered as an exceptional choice for defeating the corrosion. Carbon-steel is used in many industries due to its outstanding mechanical strength, easy accessibility, and less expensive. Though, its exposure to acidic environments results in corrosion and demanding the use of inhibitors to extend its life span and maintain structural integrity.[6] The traditional classes of inhibitors such as silicates and phosphates are effective but often pose severe health and environmental risks. The biodegradability, non-toxicity and improved effectiveness prompt to use organic inhibitors forming a protective barrier on the metal surface.[7–9] Functionalization of graphene oxide with an ionic liquid are applied as a protective coating on carbon steel and showed excellent corrosion protection efficiency.[10,11] Application of various types of corrosion control techniques and cathodic protection are frequently employed methods to subside corrosion.[12,13] Polydimethylsiloxanes (PDMS) are widely engaged as the principal coating material due to its hydrophobic nature and also protect the material from corrosion.[14] The density functional theory (DFT) simulations and electrochemical techniques applied for testing the adsorption and inhibition mechanism of azoles inhibitors on ruthenium (Ru).[15] The polymeric layer deposition on material surface will behave as a protective covering and act as an effective anticorrosive agent; however, it has several shortcomings in the form of micro-voids, exhibiting hydrophilicity to diffuse into the voids.[16] The usage of conventional corrosion inhibitors poses significant risk to the environment, and there is a need to search for eco-friendly and cost-effective alternatives.[17–21] Carbon quantum dots synthesized from waste biomass are employed as anti-corrosive coating.[22] The nanocomposite coatings of chitosan - titanium dioxide (CS/TiO_2) were employed to assess the corrosion inhibition potential of mild steel with excellent oxidation control and corrosion resistance.[23] Majority of the synthetic chemical inhibitors will lower the corrosion rate by developing a passive adsorptive layer on metal surface.[24] Novel materials and nanoparticles, nanothin layers and nanocomposites etc. have received significant scientific attention due to their attractive anticorrosive properties with enhanced surface-to-volume ratio.[25] The anticorrosive performance of CeO_2 nanoparticles displayed homogeneous distribution on metal surface exhibited outstanding corrosion resistance.[26] Novel materials and nanoparticles, nano thin layers and nanocomposites etc have received significant scientific attention due to their attractive anticorrosive properties with enhanced surface-to-volume ratio.[25] The uniform spread of nanoparticles in the polymer film exhibited superior corrosion resistance at varying compositions of nanoparticles.[27–29] The traditional corrosion inhibitors are toxic and highly expensive with reduced shelf life, obliging to the development of ecofriendly and long lasting alternatives. Therefore, it is important to develop an ecofriendly and cost effective natural protective organic coating with improved barrier properties is yet to be explored further.[30,31] Crosslinking or curing of polymer chains results in three-dimensional network structure which will enhance the chemical stability, mechanical strength, and resistance to environmental degradation thereby improves adhesion to the metal surface. Studies indicate that epoxy and amine-based cross-linked coatings exhibit superior corrosion resistance. Therefore, the incorporation of cross linking agents is considered an effective strategy for developing high-performance protective coatings for metallic materials exposed to acidic and aggressive environments.[32,33] *Ziziphus spina-christi* plants are natural medicinal plants rich in phytochemicals, and its leaves are rich in terpenoids, seanotic acids, betulinic, saponins, tannins, and other flavonoids.[34–36] The extracts of *Ziziphus spina-christi* leaves have boundless potential as an important metal based corrosion inhibitors and are nontoxic, biodegradable, environmentally friendly, and renewable. Very limited research studies have been investigated in the fabrication of green corrosion inhibitors using plant extracts, however the combination of *Ziziphus spina* plant extract, chitosan and SiO_2NPs have not been explored by the researchers. Hence, this research study examines the corrosion inhibition ability of *Ziziphus spina* extract in combination with SiO_2NPs and chitosan to develop a sustainable green inhibitor for carbon steel specimen. This interdisciplinary innovative research is well aligned with the goals and targets of United Nations Sustainable Development (UNSD-9: Industry, Innovation and Infrastructure) and supports the Oman vision 2040.

Materials and Methods

Fresh *Ziziphus spina* leaves were collected from a local estate near Muscat region of Oman. The collected leaves were cleaned thoroughly with pure water and dried under sunshade followed by grinding into fine powder. The main bioactive compounds present in the *Ziziphus spina* are flavonoids, triterpenoids, alkaloids, tannins, saponins and sterols. The medium molecular weight chitosan (Molecular weight - 200 kDa) with 85% degree of deacetylation was obtained from sigma Aldrich, India. Carbon steel samples (20 mm × 20 mm × 2 mm) are gifted by Oman Qaboos Company, Oman. The surfaces of carbon steel are polished with SiC paper to achieve a mirror-bright finish prior to ultra-sonication. Exactly 1.0 g of chitosan was dissolved in 100 ml of 1% acetic acid under stirring for two hours to form homogeneous consistency. Green synthesis technique was employed in the preparation of SiO_2NPs from neem leaves. The composite coating matrix was prepared by mixing 1% SiO_2NPs, 20 mL *Ziziphus spina* leaf extract and 10 mL chitosan and the mixing process was continued for 24 hours to achieve the required consistency. The coating process was performed by dipping the polished carbon steel specimen into the composite mixture for 10 seconds and then dried in ambient condition. The dipping was repeated for three cycles to acquire required film thickness. The uncoated and coated carbon steel coupons were exposed to different environmental conditions to study film stability. The corrosion studies were carried out by exposing the coated specimen in electrolyte solutions of 0.1 M HCl and 0.1 M NaCl. Electrochemical and weight loss measurements were performed at 30°C with carbon steel specimen fully immersed in the inhibitor solution. The specimens were weighed before and after immersion at specified intervals using a high precision electronic balance. The weight difference in ‘mg’ was noted for the initial and final weights of the carbon steel specimens.[37] All the tests were conducted at ambient conditions. The estimation of the corrosion rate is shown in Eq. (1).

$$\text{Corrosion rate} = \frac{A_1 - A_2}{s \times t \times \rho} \times 87.6 \quad \text{... (1)}$$

where, A_1 and A_2 are the weights of carbon steel specimen before and after exposure to the solutions, t is the exposure time, s is the exposure area (cm^2), and ρ is the density (g/cm^3). The density of the composite sample was measured using pycnometer method as per the Eq. (2).

$$\text{Density, } \rho = \frac{M_1 - M_2}{V} \quad \text{... (2)}$$

where, M_1 and M_2 are the weights of filled and empty pycnometer, V is the volume of the pycno meter.

The extent of corrosion performance at atomic level was observed through a high-resolution AFM (XE-100 model, Park Systems, Suwon, South Korea) and SEM (JEOL JSM-7600F). Potentiodynamic polarization measurements were carried out using a conventional three-electrode electrochemical cell connected to a CS350M electrochemical workstation (Corr Test Instruments, Wuhan, China). The electrolyte used in this study was 0.1 M HCl and NaCl (3.5% wt) solution prepared using distilled water. The working electrode was carbon steel (CS) used for the measurements. The sample dimensions were 20 mm × 20 mm × 2 mm. A saturated Ag/AgCl electrode was employed as the reference electrode, while a platinum sheet served as the counter electrode. Prior to the polarization measurements, the working electrode was immersed in the electrolyte until a stable open circuit potential (OCP) was achieved. Potentiodynamic polarization tests were performed over a potential range (-0.25 mV to 0.25 mV vs. Ag/AgCl) at a scan rate of 0.5 mV/s. The corrosion potential (E_{corr}) and corrosion current density (I_{corr}) were determined from the polarization data using the Tafel extrapolation method.

Development of Composite Coating on Carbon Steel

The fresh extract was prepared by boiling 5.0 g of *Ziziphus spina* leaf powder in 500 ml distilled water for 2 hours. After 2 hours, the solution was centrifuged at 5000 rpm for 10 min to separate the extract. The coating matrix was prepared by mixing chitosan solution, *Ziziphus spina* leaf extract, and SiO_2 NPs to obtain a homogeneous consistency. The polished carbon steel specimen was dipped in the coating solution for 10 seconds to develop a thin film on the surface. The coated carbon steel specimen was dried overnight at ambient conditions followed by stability and corrosion inhibition studies at varying environments. Fig. 1(a) shows the fresh *Ziziphus spina* leaves and Fig. 1(b) denotes the schematic of nanocomposite coating matrix preparation.

Characterization and Corrosion Inhibition Studies

The surface morphological characteristics and distribution of the prepared nanocomposite powder and nanocoating under the study was scanned through a high-resolution FE-SEM captured at voltage of 15 keV. The information on crystallite size, composition and crystallinity of the powder sample was analyzed using XRD analysis. The information

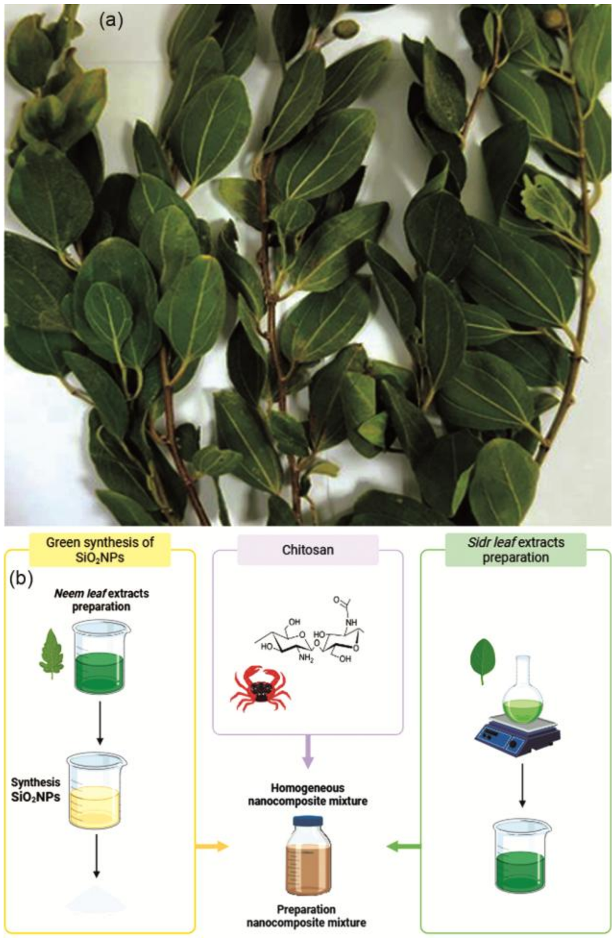

Fig. 1 — Preparation of *Ziziphus spina* - SiO_2 NPs – chitosan nanocomposite matrix: (a) Fresh *Ziziphus Spina* leaves, (b) Sequence of preparation of *Ziziphus spina* - SiO_2 NPs – chitosan nanocomposite matrix

on bond structure, chemical properties, and functional groups of the nanocomposite was recorded using FTIR spectroscopy. The surface topological features of the composite layers were monitored using AFM with nanometer precision. The corrosion inhibition studies of the specimens at varying environmental conditions are performed by immersing the coated specimen in solutions of 0.1 M NaCl and 0.1 M HCl and the coating efficiency was established using potentiostatic, dry/wet tests and atmospheric test.

Results and Discussion

The fabricated nanocomposite coating on the carbon steel specimen surface after drying was analyzed for surface morphological and microstructural characterization using a high-resolution field emission FE-SEM. The preparation of the nanocomposite coating solution is presented in Fig. 2. The Fig. 3(a) shows the morphological characteristics of the

Fig. 2 — Preparation of composite coating matrix

nanocomposite powder captured using a FE-SEM, operated at a magnification of 5000X and an excitation voltage of 15.0 keV. The morphological features in Fig. 3(a) revealed the distribution of the composite powder indicating rough and thick surface displaying high yield along with particle aggregation. The progress of coating on carbon steel coupon was analyzed to warrant the deposition and distribution of the composite matrix. The Fig. 3(b) displayed the thin layer deposition on the carbon steel surface exhibiting smooth and uniform distribution signifying the success of nanocomposite layer deposition on the specimen. The SEM image also revealed the texture and uniform surface coating shows the accomplishment of successful nanocomposite layer deposition showing more compact and uniform morphology.

The FT-IR spectroscopic assay was performed in transmittance mode to study the interaction between the SiO_2NPs, chitosan chain and the *Ziziphus spina* extract. The analysis was performed at ambient temperature with wave number ranging between 4000 cm^{-1} and 400 cm^{-1}. The FTIR spectra of fresh *Ziziphus spina* extract alone is shown in Fig. 4(a). The existence of various functional groups in the nanocomposite surface represents the bond stretching and bending vibration as illustrated in Fig. 4(b). There was a shift in the representative peaks and spectral distribution of the composite with *Ziziphus spina* extract, SiO_2NPs, and chitosan as shown in Fig. 4(b). The FTIR spectrum explains the chemical bonding between the coated layer and carbon steel surface. The representative peaks at various wave numbers endorses the specific functional groups and bond

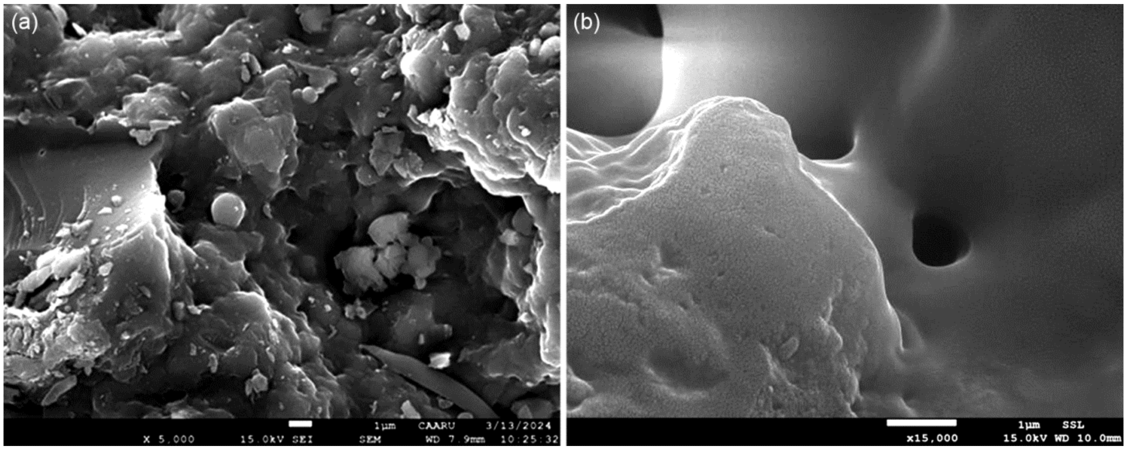

Fig. 3 — FE-SEM image of *Ziziphus spina* - SiO_2 NPs - chitosan composite: (a) powder captured at 5000X magnification, (b) coated carbon steel specimen

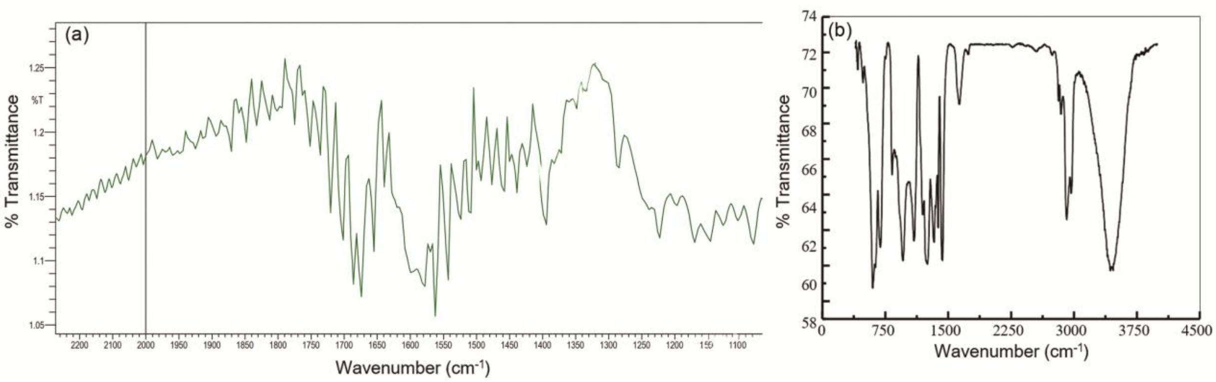

Fig. 4 — The FT-IR spectrum of: (a) Fresh *Ziziphus spina* extract, (b) nanocomposite

stretching vibrations. The peaks corresponding to 3200 – 3500 cm^{-1} in Fig. 4(b) displayed a broad band of N–H and O–H stretching. The C=O stretching at 1650 cm^{-1} is due to the presence of amide group. The silica stretching vibrations are detected at a wave number of 800 cm^{-1}. The appearance of a new band around 950–970 cm^{-1} indicates the Si–O–C bonding, endorsing the chemical interaction between chitosan, silica, and *Ziziphus spina* extract. The chemical interactions of free functional groups are due to bonding and stretching vibration, which demonstrates the coating stability and improved corrosion resistance.

The composite powder sample was used for phase identification studies and crystallographic analysis by XRD. The XRD spectrum of the nanocomposite powder given in Fig. 5 is demonstrating the composition, and crystal structure. The major crystalline peaks are displayed at 24° and 39° which show the composite formation of SiO_2NPs and chitosan. The representative peaks observed in the XRD spectrum in Fig. 5 confirm the high purity of the nanocomposite powder. The multiple peaks in the XRD spectrum indicate the increased crystallinity of the composite powder showcasing the flexibility of the polymer chain. The various diffraction peaks present in the XRD spectrum endorses the spread of nanocomposites on the carbon steel. The crystallite size is calculated using the Scherrer equation as shown in Eq. (3).

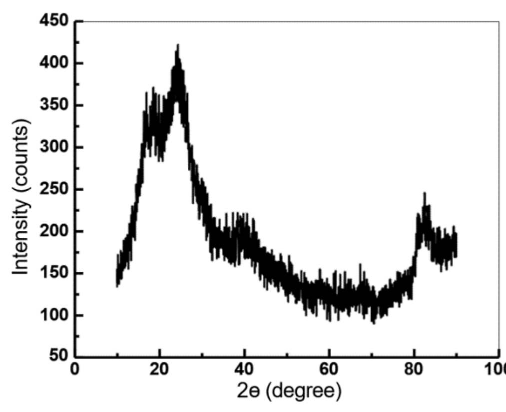

Fig. 5 — X-ray Diffractogram of the composite powder (Composition: 1% SiO_2NPs, 20 mL *Ziziphus spina* leaf extract and 10 mL chitosan)

$$d = \frac{k\lambda}{\beta \times \cos\theta} \quad \ldots (3)$$

where, d = crystallite size, λ = X-ray wavelength, β = FWHM, θ = Bragg angle. The average particle size was found to be 56 nm. The XRD analysis of the composite powder displayed good interfacial compatibility demonstrates the potential of nanocomposite to enhance corrosion resistance. The bioactive compound of *Ziziphus spina-christi* forms successful surface coverage and forms a protective binder. The complexation with phytochemicals and polymer matrix provides possible chemical interaction within the composite. This indicates that the nanocomposite forms a structurally integrated coating capable of enhancing the corrosion resistance.

The minute features of the coated film and the surface topology of the film after exposure to 0.1 M HCl and 0.1 M NaCl and the topological images were captured through AFM 3d imaging as indicated in Fig. 6(a) and Fig. 6(b). The 3D topographical study using AFM helps to analyze the compactness, identify defect-free protective layer and homogeneous nature of the nanocomposite coating on carbon steel. It was observed that the film deposition was accomplished by clear indication of rough surface and uneven distribution of coating. The topology of the nanocomposite layer reveals a dense thick layer with porous structure demonstrates the effective deposition of nanocomposite coating. The thin film was stable during the study duration. This shows the adherence of composite layers on carbon steel surface to withstand adverse environmental conditions. Fig. 6(b) reveals the rougher surface unlike the normal coating and the rms value of roughness was found to be 24 nm. The surface roughness studies and barrier properties of nano thin film using AFM surface topological imaging shows clear loops, irregular surface features, grooves and nano porous structure with enhanced roughness values.

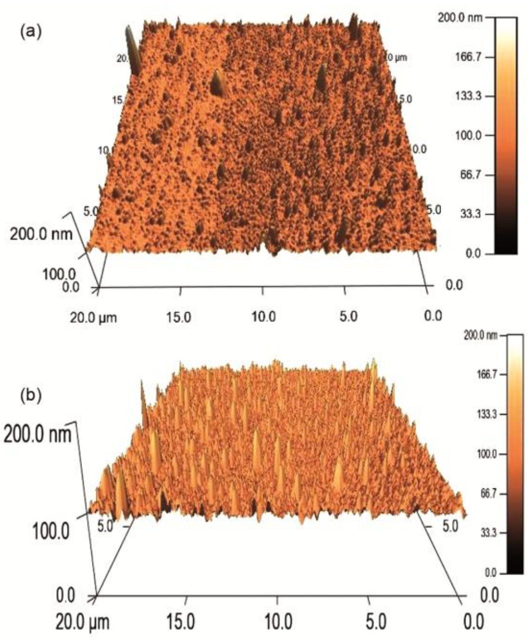

Fig. 6 — AFM 3d surface topological image of *Ziziphus spina* - SiO_2 NPs - chitosan nanocomposite coating at an exposure to: (a) 0.1 M HCl, (b) 0.1 M NaCl

The corrosion resistances of coated and uncoated carbon steel specimen are recorded for study duration of 60 days by varying the amount SiO_2NPs and the corrosion inhibition rate was calculated. The AFM imaging displays the nanoscale features and bonding between the coating and carbon steel surface, and thus correlates corrosion and barrier performance via improved adhesion. The 3D image in Fig. 6(a) reveals a densely distributed granular morphology along with nanoscale roughness exhibiting noticeable porosity and heterogeneous surface. The surface contains numerous fine grains along with isolated high-aspect-ratio. As seen in Fig. 6(b) the surface appears highly textured peaks with valleys indicating relatively high roughness owing to the aggregation of the nanoparticles and non-uniform composite film deposition on the surface. The surface topology shows increased surface area and enhanced adhesion indicating non-uniform granular growth.

The Fig. 7(a) displays the impact of variation of the amount of SiO_2 NPs on rate of corrosion. The rate decreased with augmented number of nanoparticles in the coated coupons. The AFM topological images of the nanocoating with varying dosages of SiO_2 NPs are shown in Fig. 7(b). The impact of nanocomposite with different quantities of SiO_2 NPs exposed to 0.1 M NaCl on corrosion rate is displayed in Fig. 8(a). The exposure to NaCl solution results in surface corrosion thereby affecting the structure of nanocomposites. The AFM 3d image shown in Fig. 8(b) articulates the topology of the coated carbon steel after exposure to 0.1 M NaCl. In the AFM image shown in Fig. 8(b), it was observed that any fluctuations in the roughness alter the mechanical properties thereby affecting the coating performance by the appearance of cracks and pits. The impact of variation of SiO_2 NPs dosage in nanocomposite on exposure to HCl with corrosion rate is illustrated in

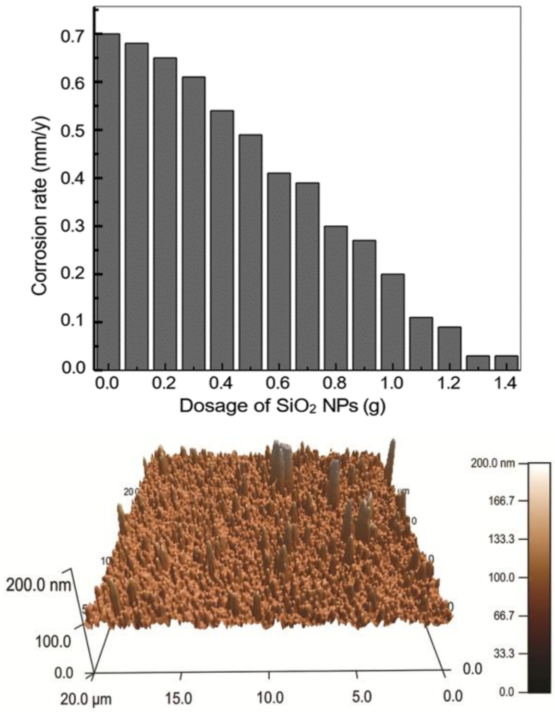

Fig. 7 — Impact of variation of SiO_2 NPs dosages on: (a) corrosion rate for coated specimen, (b) AFM 3d surface topological properties

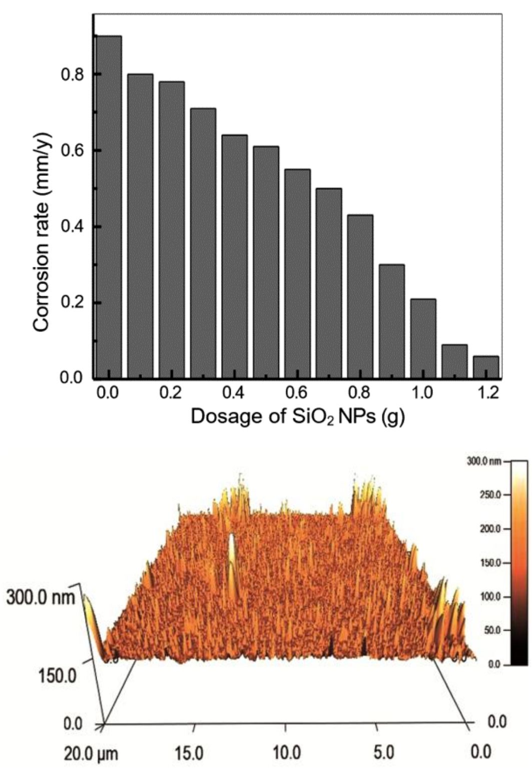

Fig. 8 — Impact of variation in dosages of SiO_2 NPs dipped in 0.1 M NaCl: (a) corrosion rate for coated specimen, (b) AFM 3d surface topological properties

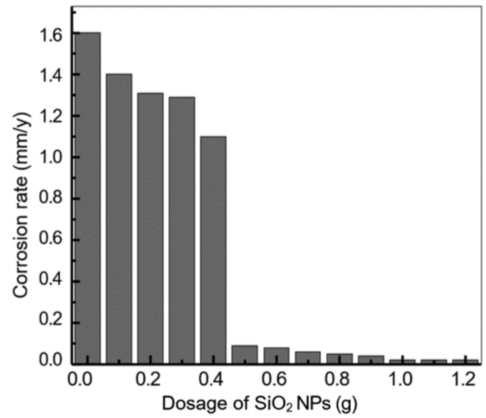

Fig. 9 — Influence of varying dosages of SiO_2 NPs in nanocomposite on corrosion rate (dipped in 0.1 M HCl)

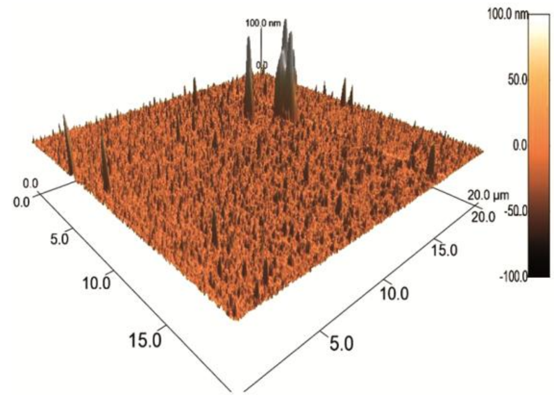

Fig. 10 — AFM 3d image of the coated specimen with varying amount of SiO_2 NPs dipped in 0.1 M H_2SO_4

Fig. 9. The coated specimen was also exposed to 0.1 M H_2SO_4 and the AFM topological characteristics are displayed in Fig. 10.

The nanocomposite coatings with varying compositions are exposed to different pH solutions for 1 hour. The results indicate that the nanocomposite layers remain intact without any observable defects like cracks, bubbles, or discoloration, indicating their stability across different pH environments. The best performance was achieved for the nanocomposite containing 1% chitosan with 0.5 g SiO_2NPs indicating improved adhesion property and viscosity. The carbon steel coated with the 1% nanocomposite shows no signs of corrosion, emphasizing the nanocomposite's stability in diverse exposure conditions. Overall, the increased amount of composite results in more robust and adhesive layers, enhancing their protective properties against adverse environmental conditions. The protective coating performance was investigated using potentiodynamic study. The potentiodynamic polarization curves of plain carbon steel and the

Table 1 — Electrochemical parameters pertinent to potentiostatic studies

Sample	Potential (E_{corr}), V	Current (I_{corr}), Amp	Anodic Tafel Slope, β_a	Cathodic Tafel Slope, β_c
Coated	−3.70	4.7 x 10^{-1}	1170	500
Uncoated	−3.80	4.3 x10^{-1}	1000	550

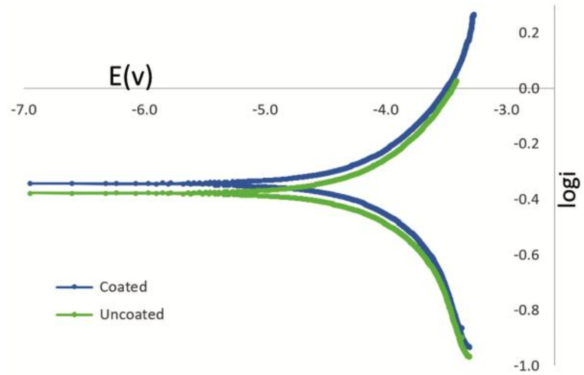

Fig. 11 — Tafel potentiodynamic plot of uncoated and *Ziziphus spina* - SiO_2NPs - chitosan nanocomposite coated carbon steel substrates

coated carbon steel after exposure to 0.1 M HCl is shown in Fig. 11. The potentiostatic studies provided the Tafel plot of bare carbon steel and nanocomposite coated carbon steel substrates exhibiting anodic and cathodic polarization curves. It is evident from Fig. 11 that the coated carbon steel shows a shift in the E_{corr} values. This positive shift indicates the enhanced corrosion resistance of coated carbon steel. Similarly, the dip in corrosion current density value further validates the superior corrosion resistance of the carbon steel. The shift in the slopes of Tafel plot is attributed to the increased distribution of composite matrix on the carbon steel surface without any aggregation thus forming a passive layer. The Tafel polarization curve displays visual insights on the corrosion behaviors and electrochemical analysis of the nanocomposite coated substrate at various corrosive environments. The green corrosion inhibitors developed from natural resources with minimum layer thickness could be a realistic solution in regulating the oil pipeline corrosion with extended life span, improved film stability, good strength, and ecofriendly approach. The electrochemical parameters from Tafel potentiodynamic plot are given in Table 1.

Conclusions

In this research, a novel and ecofriendly green corrosion inhibitor was successfully developed from *spina-christi* leaf extract, chitosan and SiO_2 NPs. The carbon steel surfaces are coated using the nanocomposite by dip coating technique. The FTIR, SEM, XRD, and AFM analyses exhibited film deposition, uniform surface finish and even distribution of the composite layer on carbon steel. The corrosion behaviors were investigated by exposing the coated specimen to different environmental conditions. The electrochemical parameters such as corrosion potential (Ecorr), corrosion current density (I_{corr}), anodic Tafel slope (β_a), and cathodic Tafel slope (β_c) etc are obtained from the Tafel potentiodynamic plot. The Galvanostatic, dry/ wet tests and atmospheric tests are well supported in the investigation on corrosion behavior of the coated specimen as evidenced by the diminishing order of corrosion rates. The coated sample showed slightly lower corrosion current density (I_{corr}) indicating improved corrosion resistance. The nanocomposite coating acts as a protective layer by preventing the metal from the attack of corrosion. The study shows that the nature of extract, exposure time and the extract concentration influences the inhibition efficiency.

Conflicts of Interest

The authors declare that they have no conflict of interest.

Acknowledgement

The authors greatly acknowledge National University of Science & Technology for providing the infrastructure facilities to perform the experiments. Also sincere thanks to Ms. Bushra Nasser Ahmed Al Sabahi, Instructor, College of Pharmacy, and Dr. Ragavesh Dandapani, College of Engineering-National University of Science & Technology for support in analysis part.

References

1 National Centre for Statistics and Information (NCSI). https://ognnews.com/Article/46837/Corrosion_in_the_oil_and_gas_industry_A_costly_challenge. Mon, 01 Jul 2024.

2 Umoren S A, Solomon M M & Saji V S, Corrosion inhibitors for sour oilfield environment (H_2S Corrosion) in *Corrosion Inhibitors in the Oil and Gas Industry* edited by Saji V S & Umoren S A (Wiley-VCH Verlag GmbH & Co. KGaA) 2020, 229–254, doi: 10.1002/9783527822140.

3 Tebbji K, FaskaN, Tounsi A & Oudda H, The effect of some lactones as inhibitors for the corrosion of mild steel in 1M

hydrochloric acid, *Mat Chem Phys*, **106** (2007) 260–267, doi: 10.1016/j.matchemphys.2007.05.046.

4 Yeganeh M, Nguyen T A, Rajendran S & Kakooei S, Corrosion protection at the nanoscale: An introduction, *Micro Nano Technol*, **4** (2020) 3–7, doi: 10.1016/B978-0-12-819359-4.00001-5.

5 Shahini H, Bahram R & Eivaz M, Recent advances in biopolymers/carbohydrate polymers as effective corrosion inhibitive macro-molecules: A review study from experimental and theoretical views, *J Molec Liq*, **325** (2021) 115110, doi: 10.1016/j.molliq.2020.115110.

6 Mehta R K, Yadav M & Obot I B, Electrochemical and computational investigation of adsorption and corrosion inhibition behavior of 2-aminobenzohydrazide derivatives at mild steel surface in 15% HCl, *Mater Chem Phys*, **290(15)** (2022) 126666, doi: 10.1016/j.matchemphys.2022.126666.

7 Mehta R K, Gupta S K Yadav, Studies on pyrimidine derivative as green corrosion inhibitor in acidic environment: Electrochemical and computational approach, *J Environ Chem Eng*, **10(5)** (2022) 108499, doi: 10.1016/ j.jece.2022.108499.

8 Sarkar T K, Yadav M & Obot I B, Mechanistic evaluation of adsorption and corrosion inhibition capabilities of novel indoline compounds for oil well/tubing steel in 15% HCl, *Chem Eng J*, **431** (2022) 13348, doi: 10.1016/ j.cej.2021.133481.

9 Chen Y, Chen Z & Zhuo Y, Newly synthesized morpholinyl Mannich bases as corrosion inhibitors for N80 steel in acid environment, *Materials*, **15(12)** (2022) 4218, doi: 10.3390/ma15124218.

10 Dhongde N R, Baranwal P K & Rajaraman P V, Functionalization of graphene oxide with an ionic liquid (1-butyl-3-methylimidazolium acetate): Preparation of epoxy-based coating on carbon steel for anticorrosive applications, *J Appl Polym Sci*, **140(27)** (2023) e54026, doi: 10.1002/app.54026.

11 Dhongde N R, Adhikari S & Rajaraman P V, Anticorrosion properties of ionic liquid functionalized graphene oxide epoxy composite coating on the carbon steel for CCUS environment, *Environ Sci Pollut Res*, **32** (2025) 4511–4522, doi: 10.1007/s11356-025-35984-6.

12 Li H, Qiang Y, Zhao W & Zhang S, 2-Mercapto-benzimidazole-inbuilt metal-organic-frameworks modified graphene oxide towards intelligent and excellent anti-corrosion coating, *Corros Sci*, **191** (2021) 109715, doi: 10.1016/j.corsci.2021.109715.

13 Zehra S, Mobin M & Aslam R, Corrosion inhibitors: An introduction in environmentally sustainable corrosion inhibitor, *Fundam Ind Appl*, **3** (2022) 47–67, doi: 10.1016/B978-0-323-85405-4.00022-7.

14 Ammar S, Ramesh K, Ma I A W, Farah Z, Vengadaesaran B & Ramesh S, Studies on SiO_2-hybrid polymeric nanocomposite coatings with superior corrosion protection and hydrophobicity, *Surf Coat Technol*, **324** (2017) 536–545, doi: 10.1016/j.surfcoat.2017.06.014.

15 Dhongde N R, Das N K, Hazarika J, Park J-G, Banerjee T & Rajaraman P V, Azoles as corrosion inhibitors in alkaline medium for ruthenium chemical mechanical planarization applications: Electrochemical and theoretical analysis, *J Molec Struct*, 1320 (2025) 139651, doi: 10.1016/j.molstruc.2024.139651

16 Guo J, Yuan S, Jiang W, Lv L, Liang B & Pehkonen S O, Polymers for combating biocorrosion, *Front Mater*, **5** (2018) 2–10, doi: 10.3389/fmats.2018.00010.

17 Ju H, Kai Z P & Li Y, Aminic nitrogen-bearing polydentate Schiff base compounds as corrosion inhibitors for iron in acidic media: A quantum chemical calculation, *Corros Sci*, **50(3)** (2008) 865–871, doi: 10.1016/j.corsci.2007.10.009.

18 Singh A K & Quraishi M A, The effect of some bis-thiadiazole derivatives on the corrosion of mild steel in hydrochloric acid, *Corros Sci*, **52(4)** (2010) 1373–1385, doi: 10.1016/j.corsci.2010.01.007.

19 Solmaz R, Investigation of the inhibition effect of 5-((E)-4-phenylbuta-1,3-dienylideneamino)-1,3,4-thiadiazole-2-thiol Schiff base on mild steel corrosion in hydrochloric acid, *Corros Sci*, **52** (2010) 3321–3330, doi: 10.1016/ j.corsci.2010.06.001.

20 Dasami P M, Parameswari K & Chitra S, Corrosion inhibition of mild steel in 1 M H_2SO_4 by thiadiazole Schiff bases, *Measurement*, **69** (2015) 195–201, doi: 10.1016/ j.measurement.2015.03.025.

21 Chauhan D S, Quraishi M A, Nik W B & Srivastava V, Triazines as a potential class of corrosion inhibitors: Present scenario, challenges and future perspectives, *J Mol Liq*, **321** (2021) 114747, doi: 10.1016/j.molliq.2020.114747.

22 Dhongde N R, Das N K, Banerjee T & Rajaram P V, Synthesis of carbon quantum dots from rice husk for anti-corrosive coating applications: Experimental and theoretical investigations, *Ind Crops Prod*, **212** (2024) 118329, doi: 10.1016/j.indcrop.2024.118329.

23 John S, Salam A, Baby A M & Joseph A, Corrosion inhibition of mild steel using chitosan / TiO_2 nanocomposite coatings, *Prog Org Coat*, **129** (2019) 254–259, doi: 10.1016/j.porgcoat.2019.01.025.

24 McCafferty E, Introduction to Corrosion Science; Springer: Berlin/Heidelberg, Germany, **1** (2010) 1–11.

25 Atta A M, El-Mahdy G A, Al-Lohedan H S & Al-Hussain, Corrosion inhibition of nanocomposite based on acrylamide copolymers /magnetite for steel, *Dig J Nanomater Biostruct*, **9(2)** (2014) 627 – 639.

26 González E, Stuhr R,Vega J M, García-Lecina E, Grande H J, Leiza J R & Paulis M, Assessing the Effect of CeO_2 nanoparticles as corrosion inhibitor in hybrid bio based waterborne acrylic direct to metal coating binders, *Polymers*, **13(6)** (2021) 848, doi: 10.3390/polym13060848.

27 Chimenti S, Vega J M, Aguirre M, García-Lecina, E, Antonio Díez J, Hans-Jurgen G, María P & Jose R Leiza, Effective incorporation of ZnO nanoparticles by miniemulsion polymerization in waterborne binders for steel corrosion protection, *J Coat Technol Res*, **14** (2017) 829–839, doi: 10.1007/s11998-017-9958-x.

28 Hosseini M G & Aboutalebi K, Improving the anticorrosive performance of epoxy coatings by embedding various percentages of unmodified and imidazole modified CeO_2 nanoparticles, *Prog Org Coat*, **122** (2018) 56–63, doi: 10.1016/j.porgcoat.2018.05.006.

29 Zhang P, Zhu M, Li W, Xu G, Huang X, Yi X, Chen J & Wu Y, Study on preparation and properties of CeO_2/epoxy resin composite coating on sintered NdFeB magnet, *J Rare Earths*, **36** (2018) 544–551, doi: 10.1016/j.jre.2017.11.012.

30 Arthur D E, Jonathan A, Ameh P O & Anya C, A review on the assessment of polymeric materials used as corrosion

inhibitor of metals and alloys, *Int J Ind Chem*, **4** (2013) 1–9, doi: 10.1186/2228-5547-4-2.

31 Devi G, Senthilkumar R & Aljabri H, Development and characterization of nanostructured thin films for corrosion control applications, In book: Novel anti-corrosion and anti-fouling coatings and thin films, **1** (2024) 323–352, doi: 10.1002/9781394234318.ch11.

32 Haldhar R, Asrafali S, Raorane C J, Periyasamy T & Kim S-C, Cross-linked PEI–epoxy polymer coatings are promising anticorrosive materials for protecting low carbon steel in aggressive acidic environments, *J Molec Liquids*, **360** (2022) 119384, doi: 10.1016/j.molliq.2022.119384.

33 Abbasi R, Mitchell A, Jessop P G & Cunningham M F, Crosslinking CO_2-switchable polymers for paints and coatings applications, *RSC Appl Polym*, **2** (2024) 214–223, doi: 10.1039/D3LP00186E.

34 Al-Ashoor S Z, Ali D S & Al-Sawaad H Z, '*Ziziphus spinachristi*' leaves methanol extract evaluation as antifungal, antibacterial, antioxidant and green inhibitor for carbon steel alloy corrosion in hydrochloric acid, *Port Electrochim Acta*, **41(2)** (2023) 167–184, doi: 10.4152/pea.2023410205.

35 Jabeen N, Maqbool Q, Sajjad S, Minhas A, Younas U, Anwaar S, Nazar M, Kausar R & Hussain S Z, Biosynthesis and characterization of nano-silica as potential system for carrying streptomycin at nano-scale drug delivery, *IET Nano Biotechnol*, **11(5)** (2017) 557–561, doi: 10.1049/iet-nbt.2016.0106.

36 Duraisamy N K, Periakaruppan R, Abed S A, Noura Al-Dayan N, Dhanasekaran S & Aldhayan S H A, Production and characterization of *Azadirachta indica*-mediated SiO_2 nanoparticles and an evaluation of their antioxidant and antimicrobial activities, *Silicon*, **2** (2023) 6663–6671, doi: 10.1007/s12633-023-02544-x.

37 Mohamed M T, Jasim AN, Nawi S A, Mustafa A M, Sayyid F F, Khadom A A, Alamiery A A, Kadhum A A H & Gaaz T S, Performance of 4-methyl-2-(1-aminoethyl)-1,3-thiazole in mitigating mild steel corrosion in hydrochloric acid, *Int J Corros Scale Inhib*, **14(1)** 2025 109–131, doi: 10.17675/2305-6894-2025-14-1-7.